# Analysis of Isothermal Turbulent Flow in a – Mechanically Ventilated Enclosure with an Obstruction.

Dr. Khudeyr S. Mushatet
College of engineering
University of Thiqar

Dr. Fadhil A. Hashim
College of engineering
University of Thiqar

Mr. Adnan A. Ugla
College of engineering
University of Thiqar

**Abstruct:**

**A numerical study to predict the distribution of air velocity, turbulence kinetic energy and static pressure inside an enclosure with obstruction is done. The characteristics of air flow are analyzed under different parameters such as location of inlet-outlet apertures and height of the obstruction. The Naries – Stockes and turbulance equations are solved using finite volume technique. The k-є model with wall function approximation is used. This work focused on study of the effect of the obstrucion on the flow disribution inside an enclosure with different locations of inlet –outlet apertures. The results show that the recirculation regions are greatly effected with the position of the inlet-outlet apertures more than the location of the obstacle. Also the results indicated that the recirculation regions are increased when the obstacle is nearest to the outlet paerture.**

## تحليل الجريان الاضطرابي داخل حيز مكيف ميكانيكياً مع وجود عائق داخل الحيز.

**المستخلص:** في هذا البحث تم إجراء دراسة عددية لتخمين توزيع سرع الهواء و الطاقة الحركية للاضطراب و الضغط الاستاتيكي داخل حيز مكيف قسرياً مع وجود عائق داخل الحيز. تم تحليل خصائص جريان الهواء تحت تاثير عوامل مختلفة مثل مواقع فتحات الدخول و الخروج و كذلك موقع و ارتفاع العائق. معادلات نافير – ستوكس و معادلات الاضطراب تم حلها باستخدام تقنية الحجم المحدد. في هذه الدراسة استخدم موديل الاضطراب ( k-є ) مع العلاقات التقريبية لدالة الجدار. بينت النتائج إن مناطق إعادة التدوير قد تأثرت بصورة كبيرة بمواقع فتحات الدخول و الخروج اكثر من تاثرها بموقع العائق. ايضاً بينت النتائج ان مناطق اعادة التدوير قد ازدادت عندما كان موقع العائق اقرب الى فتحة الخروج منه الى فتحة الدخول.

**Nomenclature:**

$h_s$ heigh of the aperture, m
H heigh of the enclosure, m

$h_{in}$ location of intlet aperture
$h_o$ location of outlet aperture
i, j tensor notation, -
k turbulance kinetic energy, $m^2/s^2$
L length of the enclosure, m
P pressure, $N/m^2$
$y_p$ distance from position p to the wall, m

Greak symbols:

$\epsilon$ turbulance dissipation rate, $m^2/s^3$
μ molecular viscosity, $N.s/m^2$
$\nu_t$ eddy viscosity, $m^2/s$
$\sigma_k$ ;$\sigma_\epsilon$ turbulent schmidt numbers, -
κ von karman constant, -
$E$ empirical constant, -
$S_\phi$ source term, -

## 1. Introduction:

There are two main ways to obtain the characteristics of the flow inside an enclosure, one is from full –scale test and the other from numerical analysis. Some papers have been published on the experimental investigation of air motion, such investigations are very expensive and detailed measured data are not available. With the development of computational fluid dynamics there is many investigations relating analysis of the flow of air inside an enclosures [1-10]. These investigations range from the prediction of air jet diffusion, air velocity and temperature distribution to fire and smoke spread inside building. The aim of this study to get an insight into the turbulent recirculating air flows inside an enclosure with obstruction under different positions of inlet-outlet apertures. Solving of the goverening equations is done numerically using finite volume techniques. This method supply us with a set of discretizations equations having algebraic form. The problem of interest is shown in Fig. 1. The size of aperture is equal to 0.2 H and the height of the obstacle equal to 0.25 H [9].

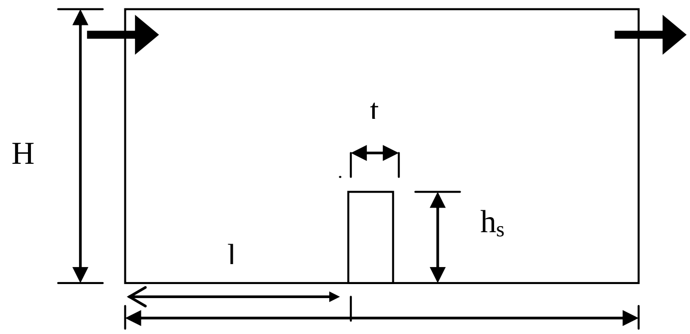


Fig.1.physical problem

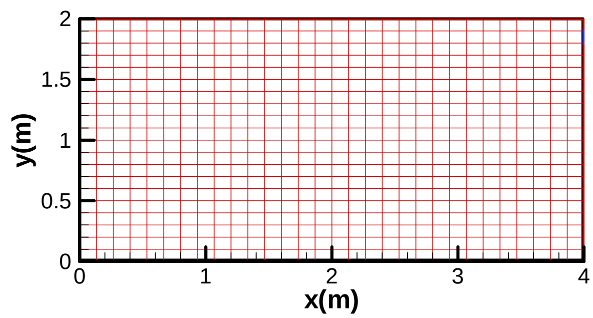


Fig.2. considered mesh

**2. Mathematical Model.**

**The instantaneous motion of turbulance flow can be mathematically solved using the conservation laws of mass and momentum. More than 250 years ago , Claude Navier and George Stokes derived the differential equations that govern the behaviour of fluid mechanics [2]. These equations are the conservation laws of momentum and the instantaneous turbulent flow field. The general form of these governing equations can be written as follows[2]:**

**Continuity equation**

$$\frac{\partial}{\partial x_i}\left(\rho \tilde{u_i}\right) = 0 \text{ ----------------------------------------------------- } \mathbf{(1)}$$

**momentum equation:**

$$\frac{\partial \tilde{u}_i \tilde{u}_j}{\partial x_j} = \frac{-\partial \tilde{p}}{\partial x_i} + \frac{\partial}{\partial x_j}\left(\mu \frac{\partial \tilde{u}_i}{\partial x_j}\right) \text{ ----------------------------------- } \mathbf{(2}$$

**The instantaneous quantity $\tilde{\phi}$ can be expressed as $\tilde{\phi} = \varphi + \phi$ , where $\varphi$ is the time averaged value and $\phi$ is the fluctuation part of $\tilde{\phi}$. After Reynolds averaging the governing equations and using the above expression of the instantaneous quantities, the equationsn have the following form:**

$$\frac{\partial}{\partial x_i}\left(\rho U_i\right) = 0 \text{------------------------------------------------------------------}(3)$$

$$\frac{\partial U_i U_j}{\partial x_j} = \frac{-\partial P}{\partial x_i} + \frac{\partial}{\partial x_j}\left(\mu \frac{\partial U_i}{\partial x_j} - \overline{\rho u_i u_j}\right) \text{-------------------------------------}(4)$$

**Where $\overline{\rho u_i u_j}$ constitute the second – moments statistical correlation or so-called Reynolds stresses.**

**2-1 Turbulance model**

**One of the most widly spread models is the standard k.є. model by Launder and Spalding [8] . This model applies two transport equations i.e. turbulent kinetic energy k and dissipation rate є , as follows:**

$$\frac{\partial \rho U_i}{\partial x_j} = \frac{\partial}{\partial x_j}\left[\left(\mu + \frac{\mu_t}{\sigma_k}\right)\frac{\partial k}{\partial x_j}\right] + \rho\left(P_k - \varepsilon\right) \text{--------------------------------}5$$

$$\frac{\partial \rho \varepsilon U_j}{\partial x_j} = \frac{\partial}{\partial x_j}\left[\left(\mu + \frac{\mu_t}{\sigma_\varepsilon}\right)\frac{\partial \varepsilon}{\partial x_j}\right] + e\frac{\varepsilon}{k}\left(C_{1\varepsilon} P_k - C_{2\varepsilon}\,\varepsilon\right) \text{-----------------------------------}6$$

**where the shear production term, ( $p_k$ ) are define as:**

$$P_k = \upsilon_t\left(\frac{\partial u_i}{\partial x_j} + \frac{\partial u_j}{\partial x_i}\right)\frac{\partial u_i}{\partial x_j} \text{----------------------------------------------------------}7$$

**and the eddy viscosity is define as:**

$$\mu_t = \rho c_\mu \frac{k^2}{\varepsilon} \text{--------------------------------------------------------------------------}8$$

**the model coefficients are ( $\sigma_k$ ; $\sigma_\epsilon$ ; $C_{1\epsilon}$ ; $C_{2\epsilon}$ ; $C\mu$) = (1.0 , 1.3 , 1.44 , 1.92, 0.09 ) respectively[8]. These coefficients are considered empirical coefficients.**

**2-2 Boundary Conditions:**

**In order to complete the mathematical model , the following boundary conditions are defined as follows according to Ref.[10]**

**At inlet**

$u = u_{in}$

$k = 0.05 u_{in}^2$

**$\epsilon = k^{1.5} / \lambda H$**

$\lambda = 0.05$

**at the walls**

**Assume no slip boundary conditions are imposed.**

$$\frac{\partial k}{\partial n} = 0$$

$$\varepsilon_p = \frac{C_\mu^{3/4} k_p^{3/2}}{\kappa y_p}$$ **; n is coordinate normal to the wall and P is a point adjacent to the wall.**

**3- Numerical Procedure**

**Finite volume method (FVM) is used to solve the above mentioned mathematical model. This gives a system of discretisation equations which means that the system of elliptic partial differential equations is transformed to the system of algebraic equations. Common Gauss-Siedl method helps in solving algebraic equations system. The essence of the discretization is to select appropriate discretization scheme (appropriate option of balance between convective and diffusion terms through the boundary of each control volume.) The general governing differential equations takes the form[11]:**

$$div(\rho U \Phi) = div(\Gamma grad \Phi) + S_\Phi \qquad \textbf{(9)}$$

**In this paper orthogonal grid with hybrid scheme is used. The one dimensional convective and diffusive fluxes can be expressed as follows:**

$$J_x = \rho U \Phi - \Gamma \frac{\partial \Phi}{\partial x} \qquad \textbf{(10)}$$

**Then by using finite volume method the discretization of east side flux by hybrid scheme gives the form [11]:**

$$\left(\rho U \Phi - \Gamma \frac{\partial \Phi}{\partial x}\right)_e = (\rho U)_e \frac{\Phi_p + \Phi_e}{2} - \Gamma_e \frac{\Phi_p + \Phi_e}{\Delta \chi_e} \qquad \textbf{(11)}$$

**A computer program is built to obtain the results of numerical procedure using SIMPLE algorithm. The first calculation is started from zero field and the every one takes the previous as initial condition.**

**4- Rsults and Discussion:**

**The results obtained from this study including velocity vectors, turbulent kinetic energy and static pressure are discussed as follow:**

**Fig 3. demonstrates the computed velocity vectors for different position of inlet-outlet aperture. It is clear that the position of aperture affected the flow behavior in all the studied cases. In case (a) the flow is characterised by the wall jet region and small recirculation region. When the air is detached from the wall, the inertia force is decreased and the velocity vectors begins to increase at the outlet aperture. A part of the flow recirculates under the effect of obstacle. There is no core region is formed in this case. In case (b) two recirculation regions are found, one in the vicinity of the wall and the other in the upper corner. The effect of obstacle on the flow is obvious. The recirculation region size is the larger among the other cases. The values of the velocity vectors are less in the vicinity of the outlet region. The semi core region is seemed to be formed at case (c) where the position of the apertures allow the flow to circulate and the inertia of the wall jet is decreased. The effect of the position of the obstacle on the flow distribution is depicted in Fig.4. As the figures show, the recirculation regions become large when the obstacle be closer**

**to the outlet aperture. This phenomina is demonated for all the studied cases. The obstacle affected the location and size of the recirculation region. Fig. 5. exihibts the effect of height of the obstacle on the flow disribution. It is clear that the recirculation region is increase in the regions adjacent to the obstacle at case (b). The validation of the numerical procedure is tested with the published experimental results as shown in Fig. 6. As the figure shows the agreement was satisfactory. Figs(7-8) shows the turbulent kinetic energy disribution under the studied cases. As Fig. 7. shows the turbulent kinetic energy is higher at case (a) among the other cases at the same location of the obstacle while in Fig. 8. the turbulent kinetic energy was higher when the obstacle is closer to the outlet aperture. The pressure disribution for the studied cases is seen in Fig.9. isobars of the studied cases indicate the pressure drop and the values of these isobars are different according to the position of aperture.**

## 6. Conclusions:

**In this work , the k-ϵ model gives acceptable results to estimate the structure of turbulent – recirculating flow inside a ventilated encloure with different positions and heights of the obstacle. The obtained results indicated that the enclosure re-circulation regions are increased when the obstacle is closer to the outlet aperture. Also the results indicated that the presence of obstacles in such kind of problems distorted the formation of central core region.**

## Refrences


1. Choi , H. L and Albright, L.D., "***Modeling the effects of obstructions in slot-ventilated enclosure***",. American society of heating , refrigeration and air conditioning engineering, Atlanta, GA., 1989.
2. Nielson, P. V, " ***flow in air conditioned rooms*** " , phd thesis, Tech. University of Denmark, 1974.
3. Zhang, J., Christianson, L.L., Wu, G.J. and Riskowski, Gl., " ***Detailed measurements of room air disribution for evaluating numerical simulation models***", ASHRAE Trasaction, 58-65, 1998.
4. Srebric , J . and Chen, Q.," ***Simplified numerical models for complex air supply diffusers***", HVAC & R Research. Vol. 8, No. 3, pp. 277-294.
5. H.T. Xu, and J.L. Niu, " ***Anew method of CFD simulation of air flow characteristics of swirling floor Diffusers***" Eighth international IBPSA conference, Nether lands, 2003.
6. Chen, Q. and Jian Z., 1992, " Significant questions in predicting room air motion, ASHRAE Transactions, vol. 98, part 1, 929-939.
7. Jones, P. J. and Whittle, G. E. , 1992, "***Comptational flui dynamics for building air flow prediction- current status and capabilities***", Building and environment, vo.. 27, pp. 321-338.
8. Launder, B. E. and Spalding, D. B., 1972**, Lecturers in Mathematical Model of Turbulence**, Academic press, London and New York.
9. Murakami, S. and Kato, S., 1989," ***Numerical and experimental study on room airflow – 3-D predictions using the k-ϵ Turbulence Model***", Building and Environment, vol. 24, n. 1, pp. 85-97.
10. Awbi, H. B, " ***Ventilation of building*** ", E. and FN spon, London(1998).
11. Suhas V. Patankar, " ***Numerical heat transfer and fluid flow*** ", 1989.

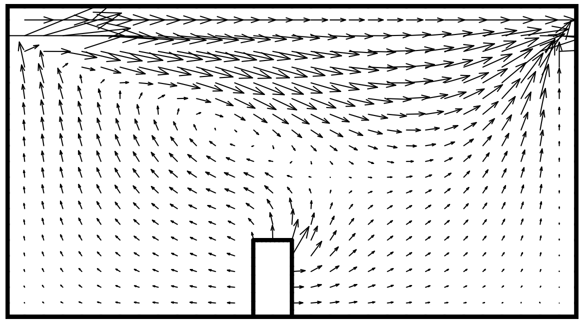

a. l=0.46L, $h_{in}$= $h_o$=0.85H

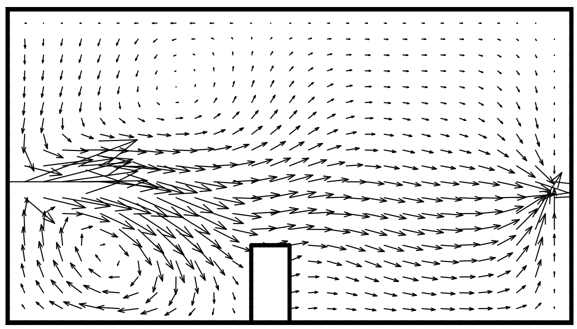

b. l=0.46L, $h_{in}$=0.46H, $h_o$=0.46H

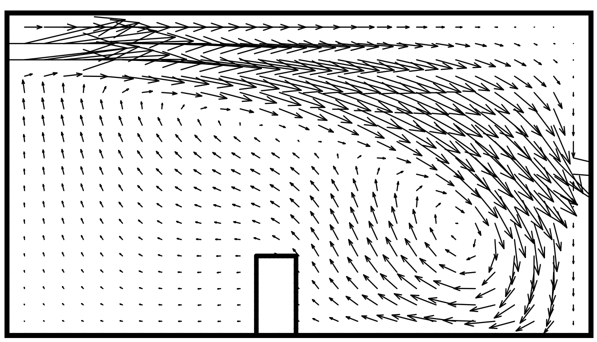

c. l=0.46L, $h_{in}$=0.85H, $h_o$=0.46H

Fig.3. predicted velocity vectors for different inlet-outlet positions

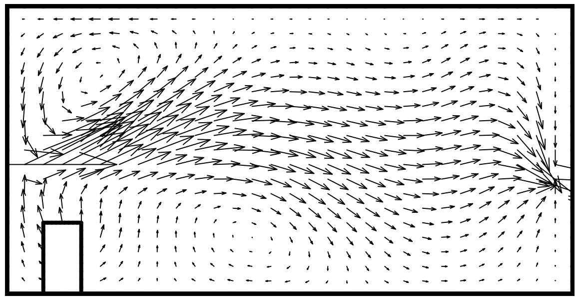

a. l=0.2L

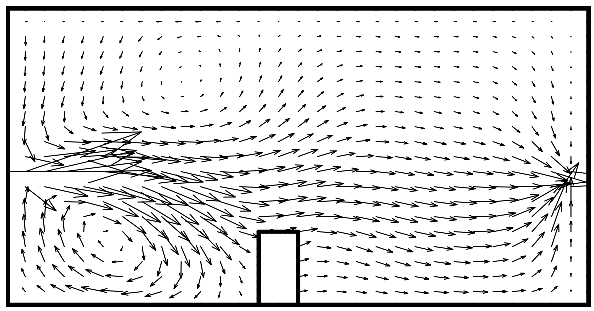

b. l=0.46L

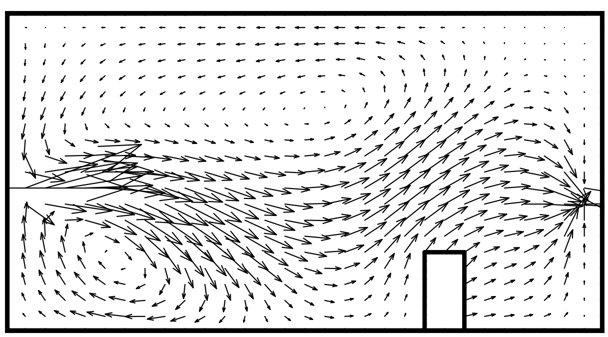

c. l=0.75L

Fig.4. predicted velocity vectors for different locations of obstruction, hs = 0.25H

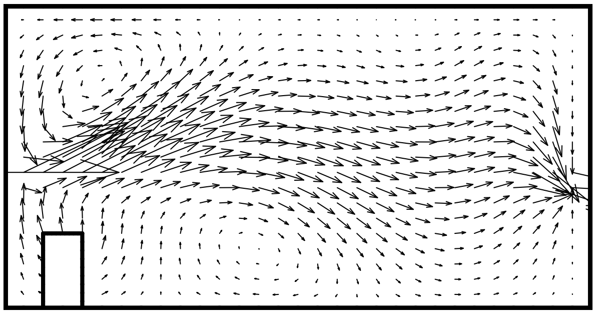

a. hs = 0.25H, l=0.2L

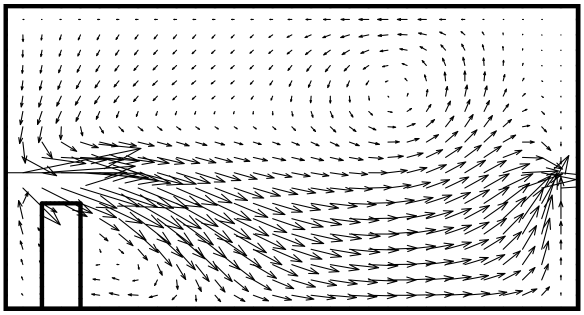

b. hs = 0.3H, l=0.2L

Fig.5. predicted velocity vectors for different heights of obstruction

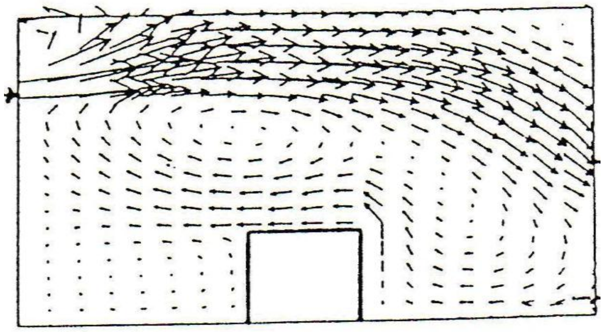

a. Experiments[17]

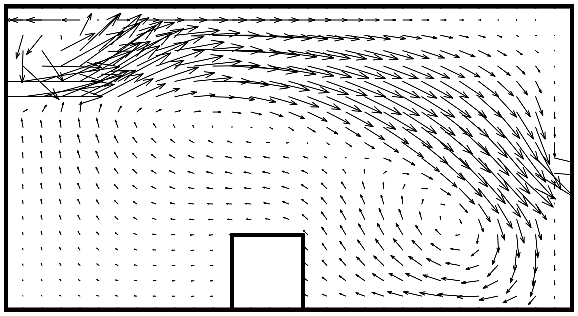

b. present prediction

Fig.6. comparison between present and published results

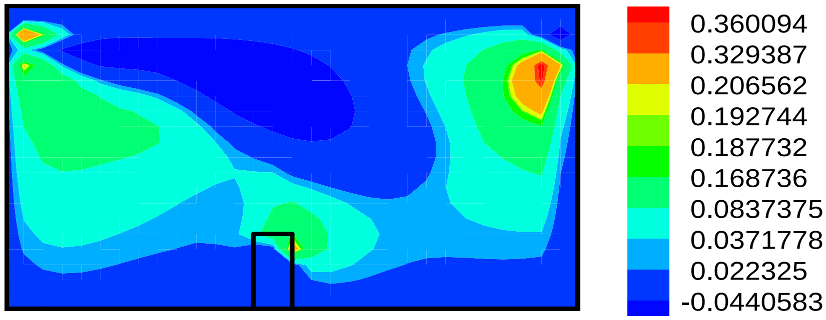


b. l=0.75L

a. l=0.46L, $h_{in}= h_o=0.85H$

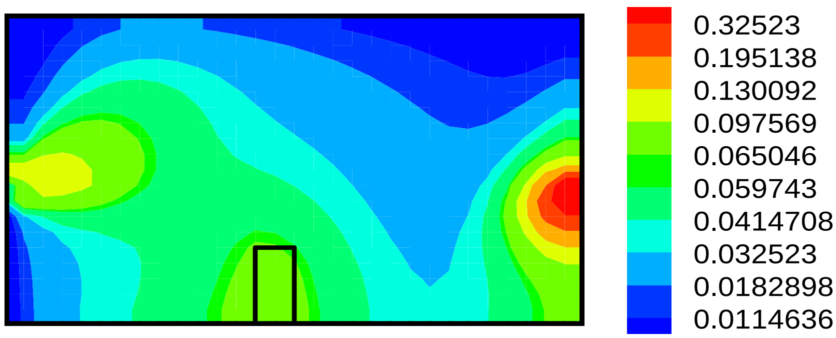


b. l=0.46L, $h_{in}= h_o=0.46H$

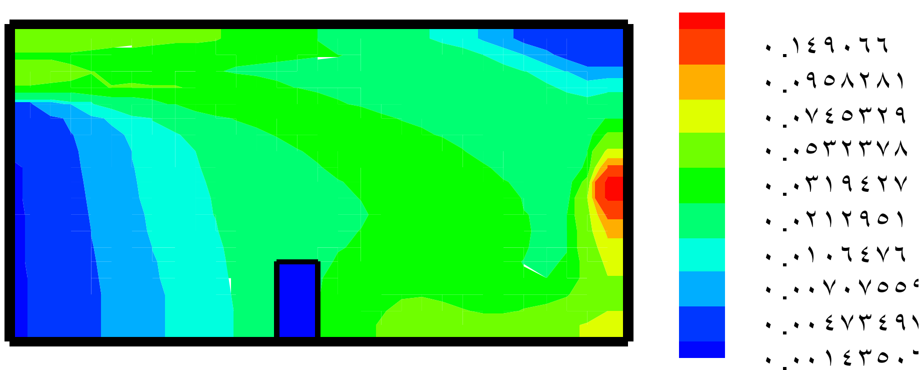


c. l=0.46L, $h_{in}=0.85H$, $h_o=0.46H$

Fig.7. Turbulent kinetic energy

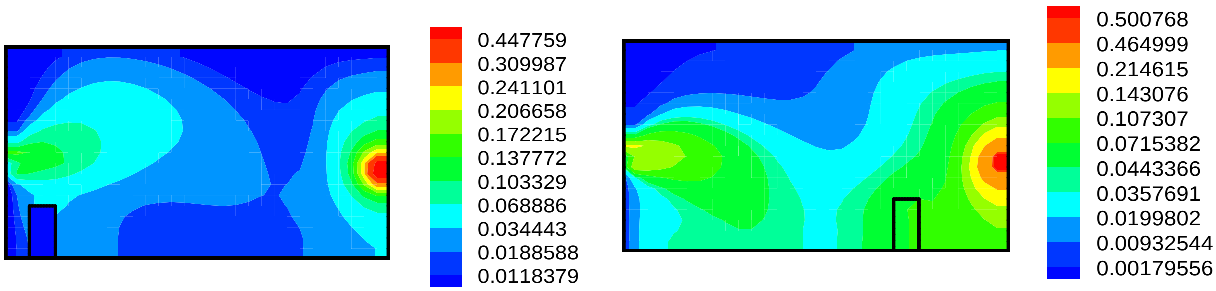


a. l=0.2L

Fig. 8. Turbulent kinetic energy for different positions

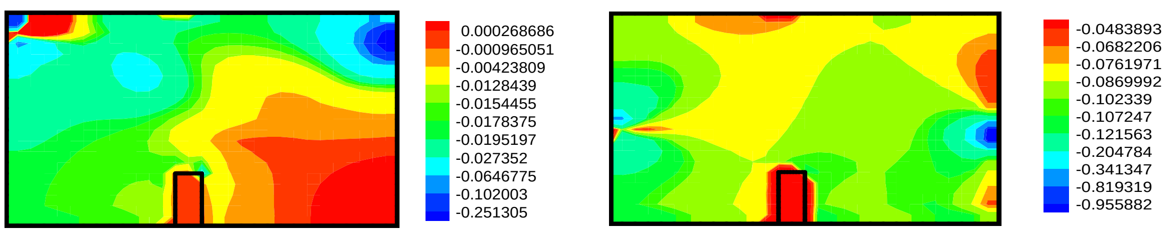


a. l=0.46L, $h_{in}$=                b. l=0.46L, $h_{in}$=0.46H,

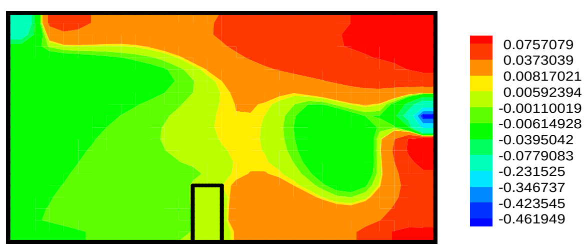


c. l=0.46L, $h_{in}$=0.85H,

Fig.9. contours of predicted Static